Anal. Bioanal. Electrochem., Vol. 10, No. 12, 2018, 1574-1586

Analytical & Bioanalytical Electrochemistry

2018 by CEE
www.abechem.com

Full Paper

Effect of Potassium Fluoride (KF) Additive on Morphology and Corrosion Behavior of Plasma Electrolytic Oxidation Films Formed on 5052 Aluminum Alloy

Azam Khodabandeloie* and Arash Fattah-alhosseini

Department of Materials Engineering, Bu-Ali Sina University, Hamedan 65178-38695, Iran

*Corresponding Author, Tel.: +988138292505; Fax: +988138257400

E-Mail: azamkhodabndeloie@yahoo.com

Received: 11 July 2018 / Accepted: 1 December 2018 / Published online: 31 December 2018

Abstract- In this study, the 5052 aluminum alloy was coated by plasma electrolytic oxidation (PEO) process in the 12 $g.l^{-1}$ sodium silicate (Na_2SiO_3. $5H_2O$), 2 $g.l^{-1}$ potassium hydroxide (KOH) using 2 $g.l^{-1}$ potassium fluoride (KF) electrolytes and also not using it. The formed films in the solutions were compared in the case of KF absence or presence in the electrolyte. The coating surface morphology was inspected using the scanning electron microscopy (SEM). Both coating composition and corrosion behavior were studied by means of X-ray diffraction (XRD) and electrochemical methods. Finally, the experimental results illustrated that having added 2 $g.l^{-1}$ KF to the electrolyte, the corrosion resistance of the coating was enhanced in addition to improving the film growth rate, despite the fact that there was no significant influence, applying varied voltages.

Keywords– PEO, 5052 aluminum alloy, Potassium fluoride, Polarization, Corrosion, Electrochemical impedance spectroscopy

1. INTRODUCTION

Aluminum and its alloys have a wide range of physical properties including low density, high specific strength, thermal, and electrical conductivities making them a suitable choice for different applications. That is why they are being widely used in many fields and their usage has been remarkably increased recently [1]. Aluminum oxides have diverse

applications in pied industrial branches such as marine and chemical industries, aerospace, automotive, biomedicine devices, electronics, energy, textile, solar cells, optics, internal combustion engines, heat exchangers, etc. [2-4].

Al alloys usage especially Al-Mg alloys in the shipbuilding [5], was considered through property/cost effectiveness. The total weight saving was estimated just over 50% after standardizing aluminum alloy components instead of steel components in marine constructions such as boats or ships. Al alloys used in marine applications have strong benefits such as lightweight, excellent corrosion resistance needing low cost for maintenance. The selection of aluminum alloys, depending on the properties/cost effectiveness of Al-Mg types that identified through the fine corrosion resistance, adhesion, formability, weld ability, manufacturing process, and in respect to the other suitable aluminum alloys avouching at least 10% lower costs for production, makes them as personable alternatives in shipbuilding for the steels [6]. For this purpose, a 5052 aluminum alloy was selected.

PEO, as a surface treatment technology, has been attracted attention to the ceramic coatings formation for valve and light metallic surfaces, e.g., Al [7,8], Mg [9-11], Ti [12-16], Zr [17] and their alloys recently. These coatings exhibit excellent properties, with potentially advantageous tribological, including high hardness, wear resistance [18-22], corrosion resistance [23-26], heat shock resistance, insulation, and thermal stability [27,28].

In fact, the PEO technique is an advanced surface modification technique that is capable of effectively depositing thick, crystalline, dense and hard oxides coatings of different compositions in aqueous solutions containing high pH. This technique performs at high voltage on light alloy substrates via an electrochemical process using localized plasma discharges, so that the electrolytic voltage exceeds the critical polarization potential of the metals and then melting–sintering occurs [29]. This phenomena only occurs in suitable electrolytes bath (low-concentrated environmental friendly alkaline electrolytes) [30,31]. Due to the requirement of severely high activation energy growth, an electrochemical cell and the PEO technique can provide strong adhesion even between ceramics and metals [32]. In these cases, the thin basic oxide layer plays the role of the intermediate layer between the soft metallic substrate and strong ceramic layer.

There are many parameters and conditions in PEO process that should be controlled in order to reach the desirable coating with suitable morphologies, composites, surface characterization, thickness, resistance behavior and simultaneous the cost-effective and environmental friend process. In some cases, researchers have improved the coating surface incorporating Nano particles [26,33].

Lugovskoy et al. studied the PEO of aluminum 5052 alloys in alkaline silicate solutions prepared by several electrolytes with different SiO_2 to Na_2O ratios of silicates [30]. In Matykina's et al. studies, the impact of incorporation of Nano particles in PEO coating was investigated [34]. Kossenko and Zinigrad determined the possibility of oxidizing aluminum

5052 and magnesium AZ91D alloys in a universal silicate base electrolyte [35]. Tseng et al. studied the additive effects on PEO coatings and the effect of sodium tungstate concentration on MAO coatings besides investigating anodizing conditions for aluminum 5052 alloy [12]. Wheeler et al. compared the microstructure and mechanical properties of hard anodized and PEO coatings on 5052 Al alloy using SEM, indentation and scratch testing [36]. In this paper, we studied the effect of KF addition to sodium silicate and potassium hydroxide electrolyte on PEO coating characterization. For this reason, a 10 $A.dm^{-2}$ DC unipolar current density was used. Moreover, the coating corrosion resistance was inspected.

2. EXPERIMENTAL PROCEDURE

2.1. PEO process

The plate of 5052 aluminum alloy (UNS A95052) with nominal composition of 2.8 wt.% Mg, 0.4wt.% Fe, 0.35wt.% Cr, 0.25wt.% Si, 0.1 wt.% Zn, 0.1wt.% Mn, 0.1wt.% Cu [37] was cut in size of 2×20×30 mm. Samples were annealed in 343 ˚C [38] for 1 hour in the furnace and then quenched in air. Before coating, samples were mechanically polished by SiC emery paper with 600, 800, 1000, 1200 and 2000 grit, and then degreased, water rinsed with distilled water and dried using cold air stream. Electrolyte components were weighed with one decimal accuracy, solvated in distilled water and stirred. The electrolyte containing 12 $g.l^{-1}$ sodium silicate (Na_2SiO_3. 5 H_2O), 2 $g.l^{-1}$ potassium hydroxide (KOH), with and without 2 $g.l^{-1}$ potassium fluoride (KF) and distilled water. The equipment for PEO consisted of a PM700/7 RC (IPS) power supply, a stainless steel receptacle, and a stirrer. The 10 Ø, 15 cm height of stainless steel receptacle used as the cathode. The electrolyte transferred to water-cooled stainless steel cathode system controlling the solution temperature below 30 ˚C throughout the experiment. The sample with nearly 20 mm of height, was vertically immersed in center of electrolyte bath strictly acting as an anode. The DC unipolar applied current density was 10 $A.cm^{-2}$ with 50 Hz frequency as the dedicated time to this treatment was 15 min. The treatment was performed under a constant current control mode. After 15 min, the process ran out, and the sample exited from the electrolyte, water rinsed, and at last immersed for 10 min in distilled water.

2.2. SEM and XRD analysis

The chemical compositions and surface morphology of each sample were observed utilizing an SEM (JEOL JSM-840A) equipped with an energy dispersive X-ray spectrometer (EDS). EDS was also used to determine the elemental composition at selected sites. For cross-section pictures, the coating samples were cut from height and mounted by epoxy resin and then polished. All the experiments were accomplished at room temperature, in addition, the reported amount was approximately an average of three times measurements. The

coatings analysis was carried out using XRD analysis with Italstructures APD2000 diffractometer using Cu Kα radiation with diffraction angle 2θ range of 10°-80° by 1°/min scanning rate and 0.05° step size. The diffractometer worked at an applied electrical current and voltage of 30 mA and 40 kV, respectively.

2.3. Electrochemical tests

To compare the corrosion behavior of the coated samples with 5052 aluminum alloy substrate, the potentiodynamic polarization and EIS tests in 3.5 wt. % NaCl solutions were carried out. After immersion, the coated sample was dried and prepared for electrochemical tests by means of μAutolab Type III/FRA2 system. For this purpose, the coated sample in 0.4 cm^2 of one surface introduced to 3.5 wt. % NaCl solution for two hours until the potential got stable. The electrochemical measurements were evaluated utilizing three different electrodes: a working electrode with 0.4 cm^2 exposed area, a reference electrode (Ag/AgCl) and a platinum counter electrode. The general corrosion behavior of the 5052 aluminum alloy having coated in silicate electrolyte was evaluated by electrochemical impedance spectroscopy (EIS) and potentiodynamic polarization tests [39]. The polarization plots were measured at a scan rate of 1 mV/s considering the open circuit potential (OCP). Moreover, EIS was conducted from 10^5 to 0.01 Hz at an interval of 36 points. The EIS and polarization tests were done respectively after OCP test.

3. RESULT AND DISCUSSION

3.1. Voltage- Time curves

As a matter of fact, the electrolytes pH was above 12 so the pH values of the electrolytes before and after PEO process (pH_1, pH_2), as can be seen in Table 1, indicated that KF augment did not make a noticeable effect.

Table 1. Samples name, composition of different electrolytes and pH of electrolytes before and after PEO treatment

Sample	Composition /g.l^{-1}			pH value	
	$Na_2SiO_3.5\ H_2O$	KOH	KF	pH_1	pH_2
A	12.0	2.0	-	12.75	13.03
A'	12.0	2.0	2.0	12.78	13.04

It implies the pH is just a bit dependent on the augment of KF [30]. It is clear that pH_1 is lower than pH_2 and may imply that amount of hydrogen ions was consumed and hydrogen

gas bubbles were released during the PEO treatment (1, 2, 4) or OH^- ions were produced due to the chemical and electrochemical reactions (1, 2).

The plasma discharge occurs through weak points such as micro cracks and pores due to the drastic electrical field. When the gas and electrolyte components ionized, instigated and splatted, the aluminum was ionized in the substrate [40-42]. The sodium is a highly reactive metal, and will immediately react and dissolve into the electrolyte (1). The reaction between the aluminum and oxygen ions caused to form the alumina ceramic coating (3). The electrical field ionized the hydrogen and silicate ions, and then silica particles produced (5) [43].

$$Na + H_2O \rightarrow Na^+ + OH^- + H_2 \uparrow \quad (1)$$

$$2H_2O + 2e^- \rightarrow H_2 \uparrow + 2OH^- \quad (2)$$

$$2Al^{3+} + 3O^{2-} \rightarrow Al_2O_3 \quad (3)$$

$$2Al + 2H_2O + 2OH^- \rightarrow 2AlO^{2-} + 3H_2 \uparrow \quad (4)$$

$$SiO_3^{2-} + 2H^+ \rightarrow SiO_2 + H_2O \quad (5)$$

The difference in Voltage- Time curves with and without KF is illustrated in Fig. 1. The shape of curves is the same in three different parts. The first part is linear with a high slope that shows the collection of ions on the surface of the substrate as the second part concerns with the dielectric break down voltage that makes discharge channels on the surface and then the voltage immediately becomes constant and saturated gradually where the third part appeared, and coating process was initialized [44]. The curves obviously reveal that the KF had no significant influence on the variations of voltages.

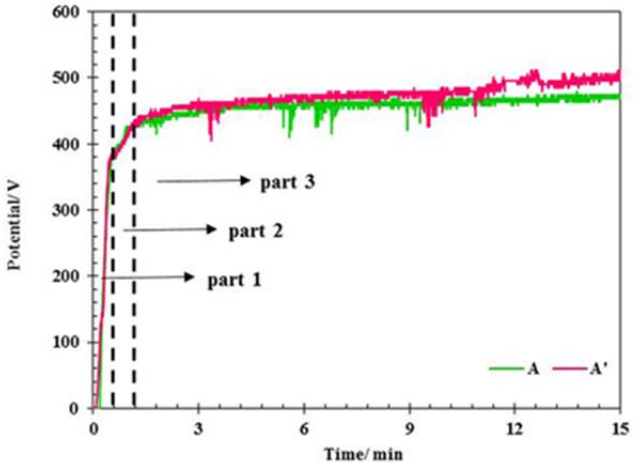

Fig. 1. Voltage-time plots of 5052 aluminum alloy samples during PEO coatings in electrolytes with and without KF addition under DC condition for 15 min applying a frequency of 50 Hz

3.2. Characteristics of PEO coatings

The SEM micrographs (Fig. 2 (a, d)) displayed the surfaces of oxide layers formed under the same PEO conditions within a couple of different electrolytes, one containing KF and the other electrolyte without it. It is obviously seen that the KF augment led to a finer and uniform structure in the coating. Also, the KF augment made the open pores of volcano-like microstructures transfer to close-overlapped volcano-like microstructures, therefore the coating resistance against corrosive media was improved (Fig. 2 (a, d)).

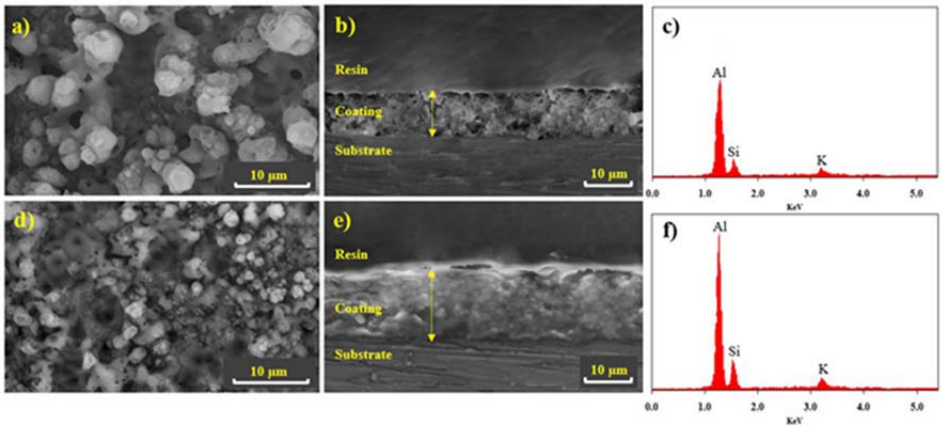

Fig. 2. Surface morphologies (a, d), cross-section images (b, e) and EDS of the oxide layer (c, f) of 5052 aluminum alloy samples with PEO coatings in presence and absence of KF in electrolytes (A, A') respectively

Cross-section analyses (Fig. 2 (b, e)) revealed that the KF augment can accelerate the formation of oxide film on account of the higher thickness of coated samples with KF than samples without KF [45]. Reaching the oxidation voltage to a critical value in weak points of the oxide film, the spark discharges possibly take place. The spark discharge channels temperature can reach to several thousand degrees. In this time, the electrolytes and aluminum substrate were overflown in the spark discharge channels and the ceramic layer was formed. Furthermore, a plenty of gases were released from spark discharge. The melted oxides were expelled with exhaust gases, therefore the spark discharge channels could not be filled by oxides so they were formed into volcano-like [44]. Increasing KF and consequently thickness, the severity of spark discharge decreases so that a reduction in the amount of the formed gases in the spark occurred. For this reason, the content of the expelled melted materials from channels decreased. In other words, more oxides were sediment at inside channels and the AlF_3 production with a low melting point (1295 °C) in comparison with other constituents, were filled the pores [45,46]. KF was conversed the larger spark discharge channels to fine spark discharges and increased the number of them. Therefore, augment of KF to electrolyte leads to homogenous and fine grain structure PEO coating [46].

The EDS issues also taken from the testing positions is illustrated in Fig. 2 (c, f). From Fig. 2(a), it was assumed that the coated samples surface morphology without KF addition in the electrolyte revealed more pores and molten oxide that was formed irregularly than the samples in the electrolyte containing KF. This occurrence was resulted from the accompaniment of micro-discharge accidental generated between the electrolyte and the aluminum substrate with electrochemical oxidation. The high plasma discharge temperatures were slumped strongly with the high cooling rate. Therefore, the oxide composites such as SiO_2 and Al_2O_3 were fabricated by reacting the anions of the electrolyte and the cations of the aluminum substrate. This depicted the presence of Al and Si in a composite that was in a good agreement with the result of EDS analysis. Conversely, in the sample that was coated with KF, few numbers of the pores were perceived. This surface of the oxide layer is shown in Fig. 2(b). This would be attributed to the effect of KF addition in filling pores. Comparing Fig. 2(c) and (f) indicates the value of Si, Al and K in the ceramic film had an increase that is related to the introduction of the KF. This indicated that the molten oxides might be mixed electrochemically with the KF in the oxide layer due to the high temperature micro-discharges, and another composition such as AlF_3 filled the pores and also Si absorption was increased in the coating layer.

The XRD pattern is shown in Fig. 3 and the four aluminum peaks are well illustrated. Meanwhile, little amount of AlF_3 and $MgAl_2O_4$ were detected besides the high amount of Al_2O_3. These results indicate that fluoride ions were participated and incorporated into the oxide coating [33] and $MgAl_2O_4$ and alumina phases were formed during PEO treatment. Also, Mg_2SiO_4 phase was formed by the interaction of substrate content with silicate ions in addition to being found the SiO_2 particles [47].

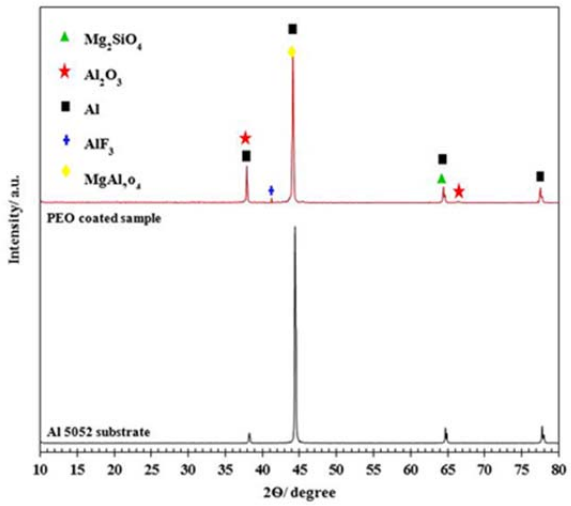

Fig. 3. XRD patterns of the 5052 aluminum alloy and PEO-coated sample in 12 $g.l^{-1}$ sodium silicate concentration, 2 $g.l^{-1}$ KOH with 2 $g.l^{-1}$ KF

3.3. Corrosion behavior of PEO coatings

The polarization plots of 5052 Al alloy by PEO coatings in the test solution are shown in Fig. 4. With linear Tafel extrapolated part of the cathodic branch back to the corrosion potential with the points more negative than E_{corr} by 50 and 100 mV the corrosion current density (i_{corr}) was calculated [48]. It was observed that the 5052 Al alloy had maximum corrosion current density, and the minimum recorded amount was for the sample A'. These conclusions indicate that the PEO process can effectively enhance the corrosion resistance of the 5052 Al alloy especially in the presence of KF additive (Table 2).

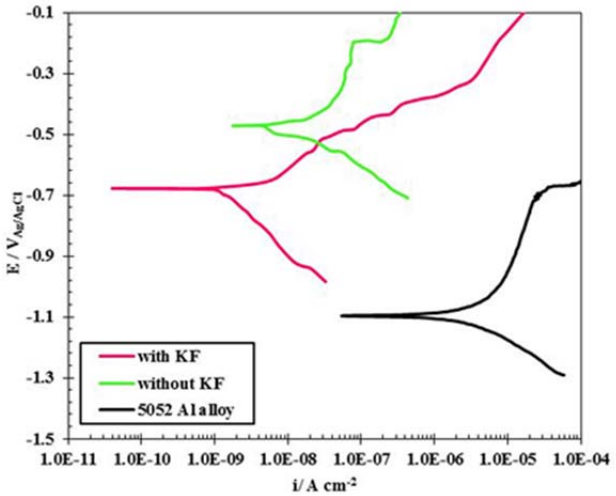

Fig. 4. Potentiodynamic polarization curves of 5052 aluminum alloy samples with PEO coatings for A, A' and base samples in the test (3.5% NaCl) solution.

This occurrence is directly concerned with the porosity percentage and pore size. Indeed, by augmenting of KF additive, the porosity percentage and the average pore size decrease. In other words, the more amount of finer micro arcs were seen in the presence of KF. Having added more KF to electrolyte led to lower corrosion potential than electrolyte without KF (Fig. 4). Moreover, the corrosion resistance was improved one order of magnitude in the presence of KF.

Table 2. Polarization parameters of coatings and bare substrate

Sample	E_{corr} /$V_{Ag/AgCl}$	i_{corr} /A.cm^{-2}
5052 Al alloy	-1.09	3.71×10^{-6}
A	-0.48	2.46×10^{-8}
A'	-0.69	7.10×10^{-9}

EIS was used to investigate the corrosion behavior of the uncoated 5052 Al alloy and PEO coated specimens. The Nyquist plots of 5052 Al alloy having PEO coatings in the test solution, is shown in Fig. 5. For as much as the Nyquist curve of uncoated 5052 Al sample, the best fitness equivalent circuit (Fig. 6(a)) was utilized.

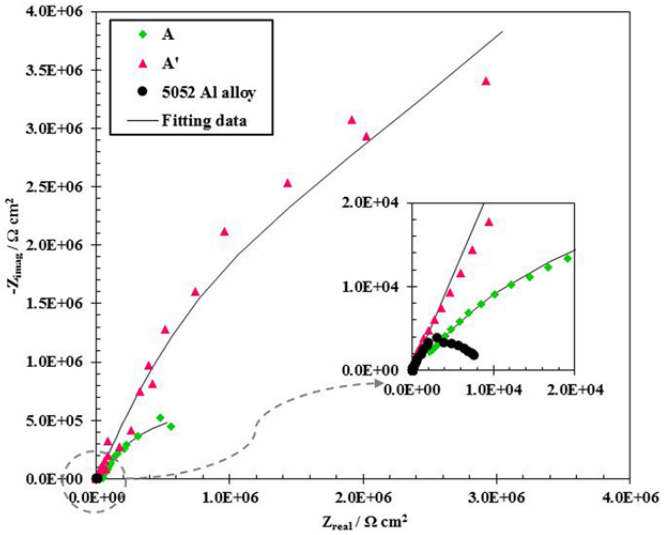

Fig. 5. Nyquist plots of 5052 aluminum alloy samples with PEO coatings for A, A' and base samples in the test solution.

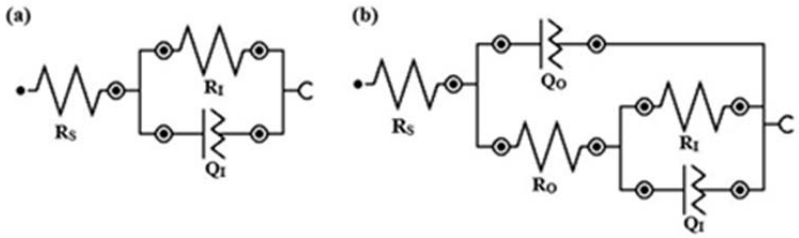

Fig. 6. Electrical equivalent circuit for the simulation of 5052 aluminum alloy with PEO coatings for A, A' and base samples

From Fig. 5, it is noteworthy that the KF coated sample displays better electrochemical efficiency than that of without KF, which is accordance to the conclusions of potentiodynamic polarization curves. To access suitable fit and estimate the surface inhomogeneity factor, a general constant phase element (Q) was used rather than a capacitive element that is denoted with (6) formula.

$$Z_Q = 1/ [(Y\ j\ \omega)^n] \quad (6)$$

Where ω is the angular frequency, j refers to the imaginary number, Z refers to the impedance of the Q, and Y and n stand for the parameters of Q. The amounts of n are between 0 and 1; that when n=1 the Q is pure capacitor [39]. In this equivalent circuit, R_s is

the solution resistance, and R_c is the charge transfer resistance of layer interface in parallel with Q_c. As observed in Fig. 6(b), a suitable equivalent circuit has been used for coated samples. In this equivalent model, R_s refers to the solution resistance, R_o is the resistance of the porous outer layer of the PEO coating which is in parallel with Q_o, and R_i is the resistance of the inner barrier layer that is in parallel with Q_i. According to an equivalent recommended circuit model, the best EIS curves fit was represented. Table 3 listed the corresponding EIS data of the equivalent circuit parameters. Despite the augment of KF, the resistance of the outer layer (R_o) was much lower than that of the inner layer (R_i). Furthermore, as a compact microstructure with less porosity has been generated in sample A', the value of resistance R_i and R_o in sample A' were more than their achieved values in sample A.

As shown in Table 3, the values of n_o and n_i in A' are higher than those in A, indicating that by the augment of KF, the interface between coating and 5052 Al alloy substrate gets smoother. The CPE-Y represented that the interface between coating and 5052 Al alloy substrate possesses dielectric behavior [35]. The amount of CPE-Y_i of the A' coated sample was lower than that of the A coating. This was concerned with the relatively thick inner coating layer in A' compared to the A (Fig .2(b) and (e)). The impedance of 5052 Al alloy is much lower than the coated samples. It indicates that the PEO improves the corrosion resistance of 5052 Al alloy effectually. The R_i of the PEO coatings is much more than the R_o. Thus it can be seen that the dense inner layer plays a major role in the 5052 Al alloy corrosion protection. Due to a much higher R_i value, all coated samples have revealed more corrosion resistant [48].

Table 3. Results of the electrochemical impedance tests of the PEO-coated samples that immersed in 3.5 wt. % NaCl solution

Sample	Fitting result					
	R_o/ kΩ cm^2	**CPE-Y_o /μF.cm^{-2}**	**CPE-n_o**	**R_i/ kΩ cm^2**	**CPE-Y_i/ μF.cm^{-2}**	**CPE-n_i**
5052 Al alloy	8.4	12.4	0.848	-	-	-
A	38.76	0.192	0.613	2024	0.639	0.721
A'	648	0.9	0.800	2652	0.109	0.738

From EIS data shown in Fig. 5, it is comprehensible that the KF enhanced the corrosion resistance that was probably concerned with the electrical conductivity rising because of ionization increment [49] and subsequently, filling of discharge channels by the form of AlF_3 phase [45,46]. The biggest chain diameter was appertained to sample A' in Fig. 5.

As can be seen in Fig. 7 the percentage of porosity was decreased when the coating carried out in the electrolyte containing KF as the percent of porosity in A and A' samples were 12.75% and 1.69%, respectively.

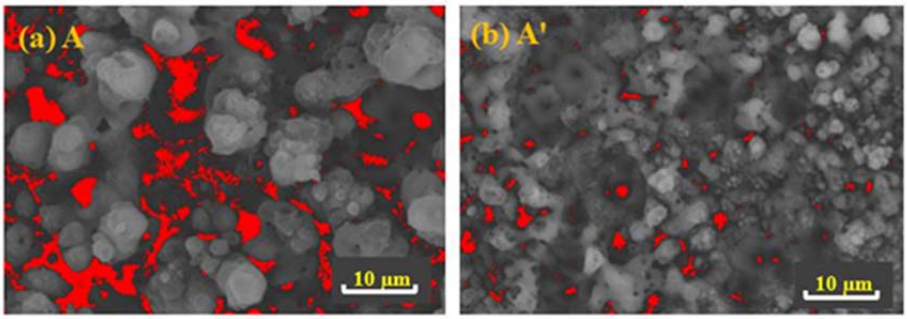

Fig. 7. The percentage of porosity in A and A' samples

4. CONCLUSION

During the PEO coating process on 5052 aluminum alloy by Na_2SiO_3. $5H_2O$, KOH and in the presence or absence of KF, the surface morphology, composition and corrosion behavior of coating were changed. The results show that the augment of KF into the electrolyte solution had no significant influence on the variations of break down voltages. In addition, adding KF to the electrolyte, the coating had a uniform and finer structure. Also, the augment of KF into the electrolyte led to a thicker coating. XRD patterns indicated that the electrolyte additives anions introduced to react with Al^{3+} that yield from the dissolution of the aluminum substrate and formed the compositions in the coating, e.g. AlF_3. In the presence of KF, much finer micro arcs were seen. Moreover, KF addition led to lower corrosion potential than the electrolyte without KF. According to EIS and polarization data, the corrosion resistance was improved one order of magnitude by KF addition.

REFERENCES

[1] J. H. Wang, M. H. Du, F. Z. Han, and J. Yang, Appl. Surf. Sci. 292 (2014) 658.

[2] D. Shen, G. Li, C. Guo, J. Zou, J. Cai, D. He, H. Ma, and F. Liu, Appl. Surf. Sci. 287 (2013) 451.

[3] Y. M. Wang, H. Tian, X. E. Shen, L. Wen, J. H. Ouyang, Y. Zhou, D. C. Jia, and L. X. Guo, Ceram. Int. 39 (2013) 2869.

[4] A. Bahramian, K. Raeissi, and A. Hakimizad, Appl. Surf. Sci. 351 (2015) 13.

[5] S. J. Kim, J. C. Park, and S. O. Chong, AME 12 (2006) 297.

[6] A. Fattah-alhosseini, S. O. Gasht, and M. Molaie, J. Mater. Eng. Perform. 27 (2018) 825.

[7] M. Vakili-Azghandi, A. Fattah-alhosseini, and M. K. Keshavarz, Measurement 124 (2018) 252.
[8] G. Y. Liu, J. Hu, Z. K. Ding, and C. Wang, Appl. Surf. Sci. 257 (2011) 2051.
[9] H. S. Ryu, and S. H. Hong, J. Electrochem. Soc. 157 (2010) 131.
[10] A. Fattah-alhosseini, and M. Sabaghi Joni, J. Mater. Eng. Perform. 24 (2015) 3444.
[11] C. Tseng, J. Lee, T. H. Kuo, S. N. Kuo, and K. H. Tseng, Surf. Coat. Technol. 206 (2012) 3437.
[12] M. Roknian, A. Fattah-alhosseini, and S. O. Gasht, J. Mater. Eng. Perform. 27 (2018) 1343.
[13] V. S. Rudnev, I.V. Lukiyanchuk, M. S. Vasilyeva, M. A. Medkov, M. V. Adigamova, and V. I. Sergienko, Surf. Coat. Technol. 307 (2016) 1219.
[14] S. Din, Y. Guo, H. Lv, J. Yu, and Z. Li, Ceram. Int. 41 (2015) 6178.
[15] S. Cheng, D. Wei, and Y. Zhou, Procedia Eng. 27 (2012) 713.
[16] Y. Chen, X. Nie, and D. O. Northwood, Surf. Coat. Technol. 205 (2010) 1774.
[17] S. Dejiu, Z. Jie, W. Lailei, L. Fangfei, L. Guolong, C. Jingrui, H. Donglei, M. Haojie, and J. Guirong, Appl. Surf. Sci., 265 (2013) 431.
[18] M. Treviño, N. F. Garza-Montes-de-Oca, A. Pérez, M. A. L. Hernández-Rodríguez, A. Juárez, and R. Colás, Surf. Coat. Technol. 206 (2012) 2213.
[19] M. Trevin˜o, R. D. Mercado-Solis, R. Cola´s, A. Pe´rez, J. Talamantes, and A. Velasco, Wear 301 (2013) 434.
[20] K. J. Ma, M. M. S. Al Bosta, and W. T. Wu, Surf. Coat. Technol. 259 (2014) 318.
[21] A. A. Voevodin, A. L. Yerokhin, V. V. Lyubimov, M. S. Donley, and J. S. Zabinski, Surf. Coat. Technol. 86-87 (1996) 516.
[22] M. Molaei, A. Fattah-alhosseini, and S. O. Gashti, Metall. Mater. Trans. A, 49A (2018) 368.
[23] A. Fattah-Alhosseini, M. Vakili-Azghandi, and M. K. Keshavarz, Acta. Metall. Sin. Engl. 29 (2016) 274.
[24] M. Roknian, A. Fattah-alhosseini, S. O. Gasht, and M. K. Keshavarz, J. Alloy. Compd. 740 (2018) 330.
[25] M. Vakili-Azghandi, A. Fattah-Alhosseini, and M. K. Keshavarz, J. Mater. Eng. Perform. 25 (2016) 5302.
[26] D. Shen, D. He, F. Liu, C. Guo, J. Cai, G. Li, and H. Ma, Ultrason. Sonochem. 54 (2014) 1065.
[27] Y. J. Liu, J. Y. Xu, W. Lin, C. Gao, J. C. Zhang, and X. H. Chen, Rev. Adv. Mater. Sci. 33 (2013) 126.
[28] Y. J. Oh, J. I. Mun, and J. H. Kim, Surf. Coat. Technol. 204 (2009) 141.
[29] A. Lugovskoy, M. Zinigrad, A. Kossenko, and B. Kazanski, Appl. Surf. Sci. 264 (2013) 743.

[30] Y. Yang, and L. Zhou, J. Mater. Sci. Technol. 12 (2014) 1251.
[31] K. M. Lee, Y. G. Ko, and D. H. Shin, Curr. Appl. Phys. 11 (2011) 255.
[32] H. X. Li, R. G. Song, and Z. G. Ji, Trans. Nonferrous Met. Soc. China 23 (2013) 406.
[33] E. Matykina, R. Arrabal, P. Skeldon, and G. E. Thompson, J. Appl. Electrochem. 38 (2008) 1375.
[34] A. Kossenko, and M. Zinigrad, Mater. Des. 88 (2015) 302.
[35] J. M. Wheeler, J. A. Curran, and S. Shrestha, Surf. Coat. Technol. 207 (2012) 480.
[36] ASM International Handbook, Properties and selection: Nonferrous alloys and special-purpose materials," ASM Met. Handb. 2 (1990) 1300.
[37] Asm International, Heat Treating, ASM Int. Mater. Park. 4 (1991) 860.
[38] M. Kaseem, M. P. Kamil, J. H. Kwon, and Y. G. Ko, Surf. Coat. Technol. 283 (2015) 268.
[39] L. Wang, L. Chen, Z. Yan, and W. Fu, Surf. Coat. Technol. 205 (2010) 1651.
[40] M. Vakili-Azghandi, and A. Fattah-alhosseini, Metall. Mater. Trans. A 48 (2017) 4681.
[41] E. V. Koroleva, G. E. Thompson, G. Hollrigl, and M. Bloeck, Corros. Sci. 41 (1999) 1475.
[42] M. S. Al Bosta, K. J. Ma, and H. H. Chien, Infrared Phys. Technol. 60 (2013) 323.
[43] H. Dong, Engineering of light alloys Aluminum, magnesium and titanium alloys, C. R. C. Press (2010).
[44] F. Liu, J. Yu, Y. Song, D. Shan, and E. H. Han, Mater. Chem. Phys. 162 (2015) 452.
[45] J. Liang, B. Guo, J. Tian, H. Liu, J. Zhou, and T. Xu, Appl. Surf. Sci. 252 (2005) 345.
[46] L. Wang, L. Chen, Z. Yan, H. Wang, and J. Peng, J. Alloy. Compd. 480 (2009) 469.
[47] M. Sabaghi Joni, and A. Fattah-Alhosseini, J. Alloy. Compd. 661 (2016) 237.
[48] S.D. Wu, H. Zhang, X.D. Dong, C.Y. Ning, A. S.L. Fok, and Y. Wang, Appl. Surf. Sci. 329 (2015) 347.